



Contents lists available at ScienceDirect

## Arabian Journal of Chemistry

journal homepage: [www.ksu.edu.sa](http://www.ksu.edu.sa)

# *Premna puberula* root petroleum ether extract inhibits proliferation, migration and invasion, and induces apoptosis through mitochondrial pathway in non-small cell lung cancer A549 cells

Nian Yang<sup>a,b,1</sup>, Xiaoyan Jia<sup>b,1</sup>, Yao Yang<sup>b</sup>, Jingming Niu<sup>c</sup>, Xia Wu<sup>a</sup>, Furong Ding<sup>a</sup>,  
Minyi Tian<sup>a,b,c,\*</sup>, Dongxin Tang<sup>c,\*</sup>

<sup>a</sup> Key Laboratory of Plant Resource Conservation and Germplasm Innovation in Mountainous Region (Ministry of Education), College of Life Sciences/Institute of Agro-bioengineering, Guizhou University, Guiyang 550025, China

<sup>b</sup> National & Local Joint Engineering Research Center for the Exploitation of Homology Resources of Southwest Medicine and Food, Guizhou University, Guiyang 550025, China

<sup>c</sup> First Affiliated Hospital of Guizhou University of Traditional Chinese Medicine, Guiyang 550000, China

## ARTICLE INFO

## Keywords:

*Premna puberula*  
Phytochemicals  
Anticancer activity  
Proliferation  
Apoptosis  
Migration and invasion

## ABSTRACT

*Premna puberula*, a medicine food homologous plant, is utilized in the preparation of cold tofu and as traditional Chinese medicine. This study aimed to identify the chemical components of *P. puberula* root petroleum ether extract (PEE) and clarify its anticancer properties and associated mechanisms. The MTT results of the four extracts (petroleum ether extract, ethyl acetate extract, n-butanol extract, and water extract) from *P. puberula* root showed that the PEE had good cytotoxic activity against A549 cells ( $IC_{50} = 38.01 \pm 3.36 \mu\text{g/mL}$ ) and low toxicity to normal cells ( $IC_{50} = 76.85 \pm 3.18 \mu\text{g/mL}$ ). The GC-FID/MS analysis revealed fifty compounds, which made up 98.6 % of the total PEE. Further antitumor assay demonstrated that PEE induced cell cycle arrest in the S phase by up-regulating p21 and cyclin E2 expression, thereby inhibiting the proliferation of A549 cells. Simultaneously, it induces apoptosis through the mitochondrial-mediated apoptosis pathway, which significantly up-regulated the ratio of Bax/Bcl-2, down-regulated mitochondrial membrane potential ( $\Delta\Psi_m$ ), promoted the release of Cyt c, activated caspase-9 and caspase-3, thereby resulting in PARP cleavage. It prevented the migration and invasion of A549 cells by reducing the expression of MMP-2 and N-cadherin. In conclusion, *P. puberula* root PEE can be a new source of antitumor agents and has significant anticancer activity *in vitro*.

## 1. Introduction

As the second most common cause of death, cancer is a serious issue for worldwide public health (She et al., 2023; Siegel et al., 2023). Globally, lung cancer remains the leading cause of cancer death, accounting for 11.4 % of cancer incidence and 18.0 % of mortality associated with cancer (Sung et al., 2021). Non-small cell lung cancer makes up 80–85 % of lung cancers (Godoy et al., 2023). Historically, natural products have greatly assisted in discovering and developing various medicines (Koehn and Carter, 2005). The commonly used anticancer drugs like vincristine, irinotecan, etoposide, and paclitaxel are sourced

from natural products (Huang et al., 2012). Natural products and their structural analogues have made major contributions to the cure of cancer (Atanasov et al., 2021). Consequently, natural products are an essential source of antitumor drugs.

*Premna puberula* Pamp. belongs to the genus *Premna* (Lamiaceae) and is a food and medicinal plant distributed in Guizhou, Guangxi, Yunnan, Sichuan, Hunan, Hubei, Guangxi, Guangdong, Gansu, and Fujian in China (Chen and Gilbert, 1994; WFO, 2023). Due to the rich pectin content, the leaf of *P. puberula* is popularly utilized in the preparation of cold tofu (commonly known as Fairy Tofu) (Xu et al., 2011; Zhang et al., 2012). As a traditional Chinese medicine, the root and stem of

Peer review under responsibility of King Saud University. Production and hosting by Elsevier.

\* Corresponding authors at: M. Tian at Key laboratory of Plant Resource Conservation and Germplasm Innovation in Mountainous Region (Ministry of Education), College of Life Sciences/Institute of Agro-bioengineering, Guizhou University, Guiyang 550025, China; D. Tang at First Affiliated Hospital of Guizhou University of Traditional Chinese Medicine, Guiyang 550000, China.

E-mail addresses: [mytian@gzu.edu.cn](mailto:mytian@gzu.edu.cn) (M. Tian), [dongxintang0319@163.com](mailto:dongxintang0319@163.com) (D. Tang).

<sup>1</sup> These authors are contributed equally to this work.

<https://doi.org/10.1016/j.arabjc.2023.105409>

Received 8 September 2023; Accepted 29 October 2023

Available online 31 October 2023

1878-5352/© 2023 The Author(s). Published by Elsevier B.V. on behalf of King Saud University. This is an open access article under the CC BY-NC-ND license (<http://creativecommons.org/licenses/by-nc-nd/4.0/>).

*P. puberula* have the effect of strengthening kidneys Yang and dispelling wind dampness and are used to treat kidney deficiency, hypertrophic spondylitis, scapulohumeral periarthritis, and irregular menstruation (Chen and Gilbert, 1994; Chinese Materia Medica Editorial Committee, 1999; Ye et al., 2022). Its leaf is utilized in the treatment of irregular menstruation, edema, malignant sores, burns, tendon injuries, and fractures; besides, its bark is boiled in water to treat toothache (Chen and Gilbert, 1994; Chinese Materia Medica Editorial Committee, 1999). Past studies have shown that the leaf and stem of *P. puberula* contain essential oils, pectin, flavonoids, and phenolics (Fu et al., 2023; Hung et al., 2020; Li et al., 2016). Its stem and leaf essential oils have been demonstrated to possess anti-inflammatory and larvicidal activities, respectively (Fu et al., 2023; Hung et al., 2020). In addition, the pectin in *P. puberula* leaf exhibits antioxidant and anti-inflammatory properties (Liu et al., 2022; Yang et al., 2022).

*P. puberula* root has been used as a traditional Chinese medicine, but its chemical constituents and pharmacological activity have not been studied. Natural products can be an excellent source of antitumor drugs. Therefore, this research aimed to investigate the chemical composition, anticancer properties and related mechanisms of *P. puberula* root PEE for the first time.

## 2. Materials and methods

### 2.1. Chemicals and reagents

Cisplatin was purchased from Aladdin Industrial Corporation (Shanghai, China). Acridine orange (AO), ethidium bromide (EB), 3-[4,5-dimethylthiazol-2-yl]-2,5 diphenyl tetrazolium bromide (MTT), 4 % paraformaldehyde, 0.1 % crystal violet solution, BCA protein assay kit were from Solarbio Life Sciences (Beijing, China). Mitochondrial membrane potential assay kit (JC-1), apoptosis Hoechst staining kit, BeyoECL moon kit, and cell mitochondrial isolation kit were bought from Beyotime Institute of Biotechnology (Shanghai, China). The cell cycle staining kit and annexin V-PE/7-AAD apoptosis kit were from MultiSciences Biotech Co., Ltd (Hangzhou, China). Cell Signaling Technology (Danvers, Massachusetts, USA) provided the antibodies, except for cytochrome c (Cyt c) and caspase-3 from Proteintech Group, Inc. (Wuhan, China). GC-MS analysis was conducted using analytical standard n-alkanes (C<sub>7</sub>-C<sub>30</sub>) provided by Merck (Darmstadt, Germany). All other reagents are analytically pure.

### 2.2. Plant material

*P. puberula* was procured in Huaxi District, Guiyang City, Guizhou Province, China, in September 2021 and identified by Prof. Guoxiong Hu, School of Life Sciences, Guizhou University. The voucher specimen (herbarium code: PP20210911) was deposited at the National & Local Joint Engineering Research Center for the Exploitation of Homology Resources of Southwest Medicine and Food, Guizhou University.

### 2.3. Preparation of extracts

The fresh root (500 g) of *P. puberula* was crushed and loaded into the round-bottom flask. Reflux extraction was performed using petroleum ether, ethyl acetate, n-butanol, and distilled water as extract solvents in sequence. During extraction with different solvents, solvent (2 L) was used for reflux extraction for 2 h and repeated twice. The collected four extracts were filtered, evaporated under decreased pressure in a rotary evaporator, and then freeze-dried. Samples of the four extracts were kept in airtight brown glass bottles and retained in a desiccator.

### 2.4. Cytotoxic activity

Non-small cell lung cancer A549 cells and fetal lung fibroblasts MRC-5 cells were obtained from Kunming Cell Bank, Chinese Academy of

Sciences (Kunming, China). Cytotoxicity was determined by MTT (Tian et al., 2020). Petroleum ether extract (PEE), ethyl acetate extract (EAE), n-butanol extract (NBE), and water extract (WE) of *P. puberula* root were applied to non-small cell lung cancer A549 cells and fetal lung fibroblasts MRC-5 cells with cisplatin as a positive control drug. *P. puberula* extract samples (50 mg) were dissolved in a 1 mL DMSO solution to prepare a mother liquor of 50 mg/mL and diluted with a culture medium. A 96-well plate with the cell suspensions (80  $\mu$ L,  $5 \times 10^3$  cells/well) was incubated at 37 °C with 5 % CO<sub>2</sub> for 24 h. After that, the cells were exposed to various doses of *P. puberula* extracts for 48 h. Subsequently, each well received 10  $\mu$ L of MTT solution, which was then incubated for an extra 4 h. After incubation, the liquid in the 96-well plate was gently aspirated with a syringe and discarded. To completely dissolve the formazan, DMSO (150  $\mu$ L) was filled in each well and oscillated for 10 min. At last, an iMark microplate reader (Bio-Rad Laboratories, Inc., Hercules, CA, USA) was used to measure the absorbance at 490 nm.

### 2.5. Composition analysis of *P. puberula* root PEE

The composition of *P. puberula* root PEE was analyzed using an Agilent 6890 gas chromatograph (GC) fitted with a flame ionization detector (FID) and an HP-5MS (60 mm  $\times$  0.25 mm, 0.25  $\mu$ m) capillary column. The flow rate of the carrier gas (helium) was 1 mL/min. Split mode (split ratio: 20:1) was used to inject 2  $\mu$ L PEE solution. The GC was operated with the following parameters: held at 70 °C for 2 min, ramped up to 180 °C at 2 °C/min (55 min), heated up to 10 °C/min to 310 °C (13 min), and kept at 310 °C for 14 min. Agilent 6890/5975C gas chromatograph-mass spectrometer (GC-MS) was used for qualitative analysis, and its GC operating parameters were identical to those in the GC-FID. The MS settings were as follows: electron energy 70 eV, ion source temperature 230 °C, interface temperature 280 °C, and mass range 29–500 amu. The relative abundance (%) of every component was computed based on the signal peak area of the FID. The n-alkanes (C<sub>8</sub>-C<sub>25</sub>) are used to determine the retention index (RI). Determination of chemical constituents in *P. puberula* root PEE was carried out by comparing the mass spectra and RI from the Wiley 275 and NIST 2020 databases.

### 2.6. Colony formation assay

A549 cells were counted, seeded at 200 cells per well in six-well plates, and cultured for 24 h. Subsequently, the *P. puberula* root PEE solution (0, 5, 10, 15, 20, 25  $\mu$ g/mL) was added, and the cultivation was continued for 48 h. Afterwards, the medium containing the drug solution was changed to a drug-free medium, and the incubation continued for 7 days. Next, staining was carried out as follows: removed medium, washed twice with PBS, fixed with 4 % paraformaldehyde solution for 30 min, discarded fixative solution, stained with 0.1 % crystal violet solution for 15 min, cleaned with water, and dried for 24 h. The clone formation rate was calculated as follows:

$$\text{Clone formation rate} = \frac{\text{Quantity of cell clones formed}}{\text{Quantity of cells inoculated}} \times 100\%$$

### 2.7. Cell cycle assay

According to the cell cycle staining kit guidelines, the cell cycle was detected. A549 cells ( $4 \times 10^5$  cells/well) in six-well plates were incubated for 24 h and treated with different concentrations of *P. puberula* root PEE solution for 24 h. After washing with PBS, cells were incubated with 10  $\mu$ L of permeabilization solution and 1 mL of DNA staining solution for 30 min under a light-avoiding environment. The ACEA NovoCyte™ flow cytometer (ACEA Biosciences, San Diego, CA, USA) was used to analyze the cell cycle distribution.

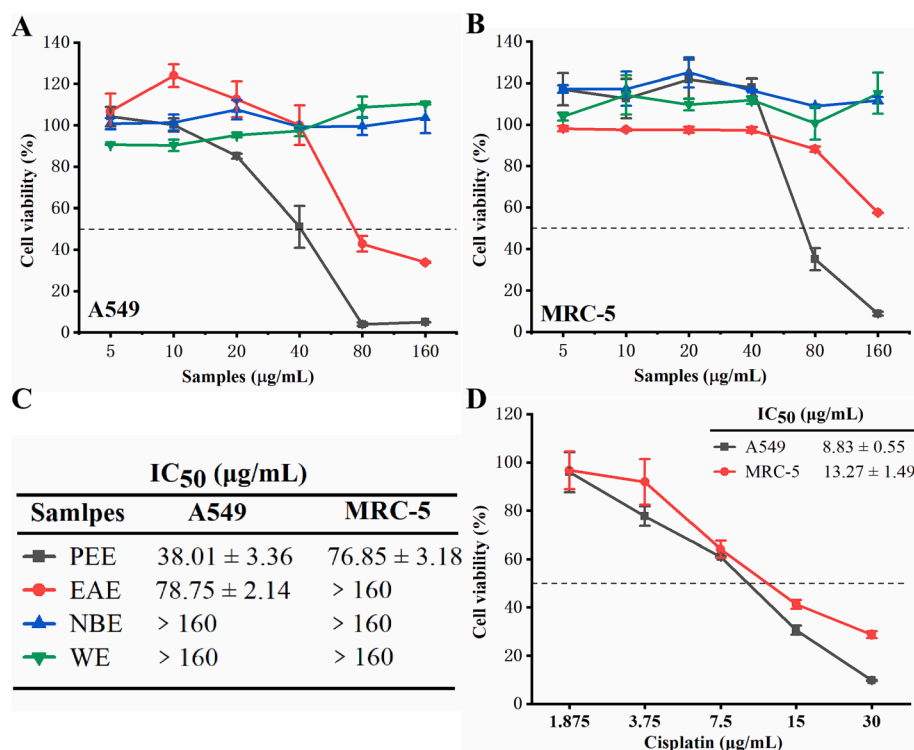


Fig. 1. (A, B) Cytotoxic activity of four extracts on A549 (A) and MRC-5 (B) cell lines. (C) The IC<sub>50</sub> values of four extracts on A549 and MRC-5 cells. (D) Cytotoxic activity of cisplatin on A549 and MRC-5 cells. IC<sub>50</sub>: Half-inhibitory concentration. Data were expressed as means ± SD.

## 2.8. Cell apoptosis assay

### 2.8.1. Morphology assay

In morphological analysis, A549 cells ( $4 \times 10^5$  cells/well) were incubated in 6-well plates and cultured for 24 h, followed by treatment with medium containing 0, 40, 60, 80, and 100 μg/mL of *P. puberula* root PEE. After 48 h of culture, the Leica DMi8 microscope (Leica Microsystems, Germany) was used to observe the morphological alterations in A549 cells.

In AO/EB staining assay, A549 cells were treated with the aforementioned procedure. After discarding the supernatant, cells were washed twice with PBS and stained with AO/EB mixture (100 μg/mL, 1 mL) for 5 min in the absence of light. Next, cells were observed under a fluorescence microscope.

A549 cells were treated as above in the Hoechst 33,258 staining assay. After removing the medium, cells were fixed with 500 μL 4 % paraformaldehyde solution for 10 min, washed twice with PBS, and stained with 500 μL of Hoechst 33,258 for 5 min. Finally, the staining solution was discarded and washed twice with PBS to observe the morphological changes of the nucleus by fluorescence microscopy.

### 2.8.2. Annexin V-PE/7-AAD assay

A549 cell apoptosis was quantitatively estimated using an Annexin V-PE/7-AAD apoptosis kit. Briefly, A549 cells ( $3 \times 10^5$  cells per well) in 6-well plates were cultured for 24 h and then exposed to 0, 20, 40, 60, 80, and 100 μg/mL of *P. puberula* root PEE solutions for 48 h. After centrifuging and washing in pre-cooled PBS, cells were collected and resuspended in  $1 \times$  Binding Buffer (500 μL). Then, cells were stained with 5 μL Annexin V-PE and 10 μL 7-AAD, gently vortexed, and incubated at room temperature for 5 min while shielded from light. The flow cytometer was used to detect the apoptosis rate.

## 2.9. JC-1 staining

The mitochondrial membrane potential assay kit was used to

determine the membrane potential of the mitochondria. The A549 cell suspensions ( $4 \times 10^5$  cells/well) were incubated in six-well plates for 24 h. At the end of incubation, each well was treated with corresponding concentrations (0, 20, 40, 60, 80, and 100 μg/mL) of *P. puberula* root PEE solution. After 48 h incubation, the medium containing the drug solution was discarded, and 900 μL of medium and 900 μL of JC-1 working solution were added. The six-well plate was put back into the incubator for 20 min. Finally, the cells were observed using an inverted fluorescent microscope after being washed twice with JC-1 staining buffer.

## 2.10. Cell migration and invasion assay

### 2.10.1. Wound healing assay

The wound healing assay was conducted to evaluate the effect of PEE on cell migration ability (Hong et al., 2022). The A549 cell suspensions (2 mL,  $2 \times 10^5$  cells/mL) were added to each well of 6-well plates. Cells were incubated until they spread across the bottom of the six-well plate to form a monolayer of fused cells. Then, a straight line was drawn on the monolayer cells of each well with the tip of a 200 μL pipette. Next, the floating cells were washed away with PBS, and then different concentrations of *P. puberula* root PEE solutions (serum-free medium preparation, 2 mL) were added and incubated for 48 h. A Leica microscope was used to take pictures of the scratch at 0 and 48 h. Cell migration rates were calculated as follows:

$$\text{Migration rate} = \frac{S_{\text{scratch area of 0 h}} - S_{\text{scratch area of 48 h}}}{S_{\text{scratch area of 0 h}}} \times 100\%$$

### 2.10.2. Transwell invasion assay

The Corning® BioCoat™ Matrigel® invasion chamber (Corning, New York, USA) was utilized for the transwell invasion assay. The lower chamber was injected with 750 μL of 15 % FBS medium containing different concentrations of PEE. The 5 % FBS medium (250 μL) containing A549 cells ( $1 \times 10^5$  cells per well) and various doses of PEE solutions (dissolved in 5 % FBS medium, 250 μL) were loaded into the upper chamber. At the end of 48 h incubation, cells were fixed with 4 %

**Table 1**  
Chemical components of the PEE from *P. puberula* root.

Compounds	RT <sup>a</sup>	RI <sup>b</sup>	RI <sup>c</sup>	Area (%)	CAS	Identification <sup>d</sup>
Hexanal	7.58	802	801	0.2	000066–25-1	MS, RI
2,4-Dimethylheptane	8.09	819	821	0.1	002213–23-2	MS, RI
4-Methyloctane	9.33	858	863	0.1	002216–34-4	MS, RI
Heptanal	10.76	903	901	0.4	000111–71-7	MS, RI
<i>p</i> -Cymene	16.82	1027	1025	0.1	000099–87-6	MS, RI
Eucalyptol	17.27	1035	1032	0.5	000470–82-6	MS, RI
4,5-Dimethylnonane	18.50	1056	1046	0.2	017302–23-7	MS, RI
<i>o</i> -Isopropylanisole	20.14	1084	1118	4.3	002944–47-0	MS, RI
Nonanal	21.39	1105	1104	0.2	000124–19-6	MS, RI
2-Methyldecalin	23.13	1132	1129	0.1	002958–76-1	MS, RI
1-Methyldecalin	23.62	1139	1134	0.1	002958–75-0	MS, RI
1-Dodecene	26.89	1190	1190	0.2	000112–41-4	MS, RI
Dodecene	27.44	1199	1200	0.2	000112–40-3	MS, RI
Tridecene	33.98	1299	1300	0.5	000629–50-5	MS, RI
$\alpha$ -Cubebene	37.55	1355	1351	0.3	017699–14-8	MS, RI
Cyclosativene	38.86	1375	1368	12.0	022469–52-9	MS, RI
$\alpha$ -Copaene	39.32	1382	1376	5.0	003856–25-5	MS, RI
1-Tetradecene	39.88	1391	1392	0.6	001120–36-1	MS, RI
Tetradecane	40.37	1399	1400	0.4	000629–59-4	MS, RI
(+)-Sativene	40.69	1404	1396	1.1	003650–28-0	MS, RI
$\alpha$ -Gurjunene	41.50	1417	1409	0.3	000489–40-7	MS, RI
Eremophilene	46.30	1495	1494	0.5	010219–75-7	MS, RI
$\alpha$ -Selinene	46.79	1503	1494	2.5	000473–13-2	MS, RI
$\alpha$ -Muurolene	46.97	1506	1499	0.6	010208–80-7	MS, RI
2,4-Di- <i>tert</i> -butylphenol	47.41	1514	1514	0.7	000096–76-4	MS, RI
$\delta$ -Cadinene	48.35	1530	1524	1.9	000483–76-1	MS, RI
$\alpha$ -Calacorene	49.60	1551	1542	2.7	021391–99-1	MS, RI
$\beta$ -Calacorene	50.78	1571	1563	0.2	050277–34-4	MS, RI
Spathulenol	51.77	1588	1576	0.8	006750–60-3	MS, RI
Cetene	51.96	1591	1592	0.8	000629–73-2	MS, RI
Caryophyllene oxide	52.08	1593	1581	4.4	001139–30-6	MS, RI
Viridiflorol	52.62	1603	1591	1.2	000552–02-3	MS, RI
Humulene epoxide I	52.95	1609	1604	0.8	019888–33-6	MS, RI
Humulene epoxide II	53.59	1620	1606	7.6	019888–34-7	MS, RI
Copaborneol	54.40	1635	1623	0.8	021966–93-8	MS, RI
$\alpha$ -Cadinol	55.35	1652	1653	2.1	000481–34-5	MS, RI
Humuleneol-II	55.58	1657	1650	0.3	019888–00-7	MS, RI
$\beta$ -Eudesmol	55.92	1663	1649	0.9	000473–15-4	MS, RI
$\alpha$ -Eudesmol	56.06	1665	1653	1.4	000473–16-5	MS, RI
Ylangenal	56.49	1673	1675	0.2	041610–68-8	MS, RI
Cadalene	57.14	1685	1674	2.0	000483–78-3	MS, RI
1-Octadecene	61.09	1793	1793	2.7	000112–88-9	MS, RI
<i>trans</i> -5-Octadecene	61.27	1799	1801	0.5	007206–21-5	MS, RI
Isopimara-9(11),15-diene	64.17	1938	1906	1.3	039702–28-8	MS, RI
3-Eicosene	65.10	1993	1999	3.9	074685–33-9	MS, RI
Dehydroabietan	66.43	2088	2075	4.2	019407–28-4	MS, RI
1-Docosene	67.68	2194	2194	4.3	001599–67-3	MS, RI
Tricosane	68.77	2299	2300	2.4	000638–67-5	MS, RI
Ferruginol	69.56	2383	2325	15.0	000514–62-5	MS, RI
Pentacosane	70.59	2498	2500	5.2	000629–99-2	MS, RI
Total (%)				98.6		

<sup>a</sup> RT: Retention times.

<sup>b</sup> RI (Retention indices) were computed using the n-alkanes (C<sub>8</sub>–C<sub>25</sub>).

<sup>c</sup> RI from databases (NIST 2020 and Wiley 275).

<sup>d</sup> Identification: MS, using databases (NIST 2020 and Wiley 275) to match MS similarity; RI, comparing calculated RI with those in databases (NIST 2020 and Wiley 275).

paraformaldehyde for 2 min, incubated with anhydrous methanol for 20 min, and colored with 0.1 % crystal violet for 15 min. The pictures were recorded by a Leica DMi8 microscope after rinsing with PBS twice, and the count of invasive cells per field of view was performed using Image J software.

### 2.11. Western blotting assay

A549 cells in six-well plates ( $4 \times 10^5$  cells/well) were cultivated at 37 °C for 24 h and were exposed to various concentrations of *P. puberula* root PEE solution for 48 h. Total protein concentration was determined using a BCA kit after extraction of total protein using radio-immunoprecipitation assay (RIPA) lysis buffer. The protein was then transferred to a PVDF membrane after being separated with 10 % SDS-

PAGE. The PVDF membranes were closed in TBST containing 5 % skimmed milk powder for 1 h and incubated with the primary antibody overnight at 4 °C. Subsequently, the membranes were washed three times (5 min each) with TBST and incubated with secondary antibody for 1 h. After washing the membranes three times with TBST for 5 min each time, chemiluminescence was carried out, and the Image Lab software (Bio-Rad, CA, USA) was used for quantification.

### 2.12. Statistical analysis

The mean  $\pm$  standard deviation (SD) from at least three experiments was used to represent all data. The SPSS 25.0 software was used for the statistical analysis. The significant difference between the two groups was compared via Dunnett's test and one-way analysis of variance

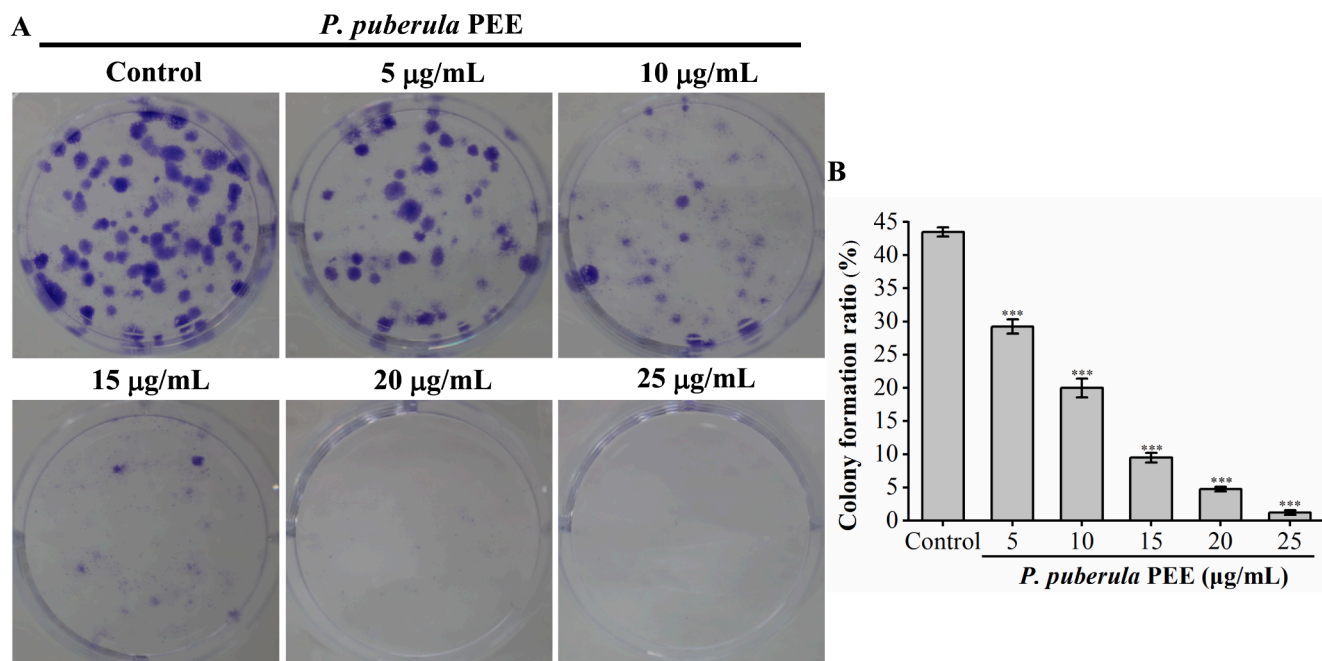


**Fig. 2.** *P. puberula* root PEE's inhibitory effect on A549 cell colony formation. A549 cells (200 cells/well) were inoculated in a six-well plate containing *P. puberula* root PEE for 7 days. (A) The images show representative crystal violet-stained A549 cell colonies. (B) A549 cell colony formation rate (%). Data were presented as means  $\pm$  SD. \*\*\*  $p < 0.001$  versus the control group. (For interpretation of the references to colour in this figure legend, the reader is referred to the web version of this article.)

(ANOVA) at \* $p < 0.05$ , \*\* $p < 0.01$ , and \*\*\* $p < 0.001$ .

### 3. Results

#### 3.1. Cytotoxic activity of *P. puberula*

The cytotoxic activity of these four extracts against A549 and MRC-5 was detected by MTT, with cisplatin as a positive control drug. Among the four *P. puberula* root extracts, PEE exhibited the most potent cytotoxicity against A549 with an  $IC_{50}$  of  $38.01 \pm 3.36$  µg/mL than the remaining three extracts (Fig. 1A and C). In addition, as shown in Fig. 1B and C, *P. puberula* root PEE revealed less cytotoxicity on non-cancerous MRC-5 cells ( $IC_{50} = 76.85 \pm 3.18$  µg/mL) compared to A549 cancer cells. These results indicated that *P. puberula* root PEE had a selective cytotoxic effect on non-small cell lung cancer A549 cells. Therefore, *P. puberula* root PEE was selected for subsequent research on anti-A549 lung cancer cell effects.

#### 3.2. Chemical compounds of *P. puberula* root PEE

The extraction rates of *P. puberula* root PEE, EAE, NBE, and WE were 0.14 %, 0.68 %, 0.52 %, and 5.84 %, respectively. As shown in Table 1, GC-FID/MS identified 50 chemical components, accounting for 98.6 % of the *P. puberula* root PEE. The main constituents were ferruginol (15.0 %), cyclosativene (12.0 %), humulene epoxide II (7.6 %), pentacosane (5.2 %),  $\alpha$ -copaene (5.0 %), caryophyllene oxide (4.4 %), *o*-isopropylanisole (4.3 %), 1-docosene (4.3 %), dehydroabietan (4.2 %), and 3-eicosene (3.9 %).

#### 3.3. *P. puberula* root PEE's inhibitory effects on colony formation

The inhibitory impact of *P. puberula* root PEE on the proliferation of A549 cells was examined by colony formation assay. A549 cell colonies were significantly decreased in size and quantity by *P. puberula* root PEE in a dose-dependent manner (Fig. 2). In comparison to the untreated group ( $43.50 \pm 0.71$  %), the clone formation rates of A549 cells treated

with different concentrations of *P. puberula* root PEE (5 µg/mL, 10 µg/mL, 15 µg/mL, 20 µg/mL, and 25 µg/mL) were significantly reduced to  $29.25 \pm 1.06$  %,  $20.00 \pm 1.41$  %,  $9.50 \pm 0.71$  %,  $4.75 \pm 0.35$  %, and  $1.25 \pm 0.35$  %, respectively. According to the aforementioned findings, *P. puberula* root PEE significantly inhibited the proliferation of A549 cells.

#### 3.4. *P. puberula* root PEE induced S phase cell cycle arrest

The deregulation of the cell cycle can result in unrestricted proliferation of cancer cells (Diaz-Moralli et al., 2013). An analysis of the cell cycle was performed to ascertain whether the antiproliferative effect of *P. puberula* root PEE was caused by cell cycle arrest. As seen in Fig. 3, after treatment with *P. puberula* root PEE at concentrations of 0, 20, 40, 60, 80, and 100 µg/mL, the proportion of cells in the S phase increased from  $37.53 \pm 0.83$  % in the control group to  $39.88 \pm 0.74$  %,  $46.08 \pm 0.14$  %,  $50.62 \pm 0.96$  %,  $56.93 \pm 0.45$  %,  $57.55 \pm 1.05$  %, respectively. Western blot was used to detect proteins related to the regulation of S phase cell cycle progression. As shown in Fig. 3C and D, after *P. puberula* root PEE treatment, the expression of p21 was significantly and dose-dependently upregulated. Besides, *P. puberula* root PEE markedly increased cyclin E2 level at 60 and 80 µg/mL. The results showed that *P. puberula* root PEE induced S cell cycle arrest by up-regulating p21 and cyclin E2 expression and thus inhibited the proliferation of A549 cells.

#### 3.5. *P. puberula* root PEE induced apoptosis of A549 cells

The A549 cells treated with *P. puberula* root PEE displayed the characteristic morphological changes of apoptosis, such as shrinkage and cell rounding (Fig. 4A). In addition, AO/EB staining and Hoechst 33,258 staining were used to determine the nuclear morphological changes and to further explore the apoptosis of A549 cells induced by *P. puberula* root PEE. In Fig. 4B, AO/EB staining results indicated that the proportion of nuclei showing orange-red fluorescence gradually up-regulated with rising PEE concentration, indicating that apoptotic cells gradually increased. In Fig. 4C, Hoechst 33,258 staining results

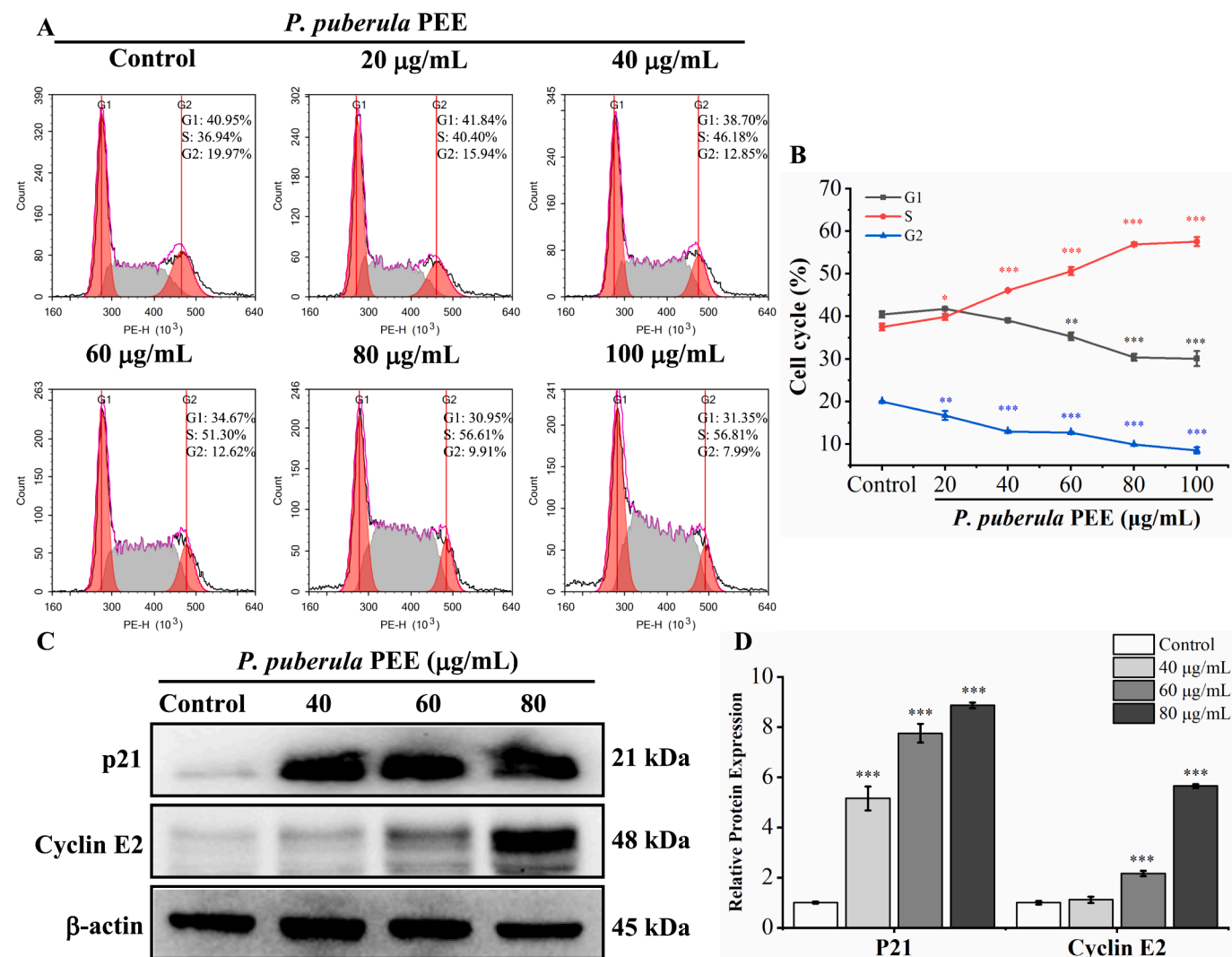


**Fig. 3.** Cell cycle was arrested in the S phase by *P. puberula* root PEE. (A) The distribution of the cell cycle in A549 cells treated with *P. puberula* root PEE was determined by flow cytometry. (B) The proportion of cells in the G1, S, and G2 phases. (C) Western blot detection of p21 and cyclin E2 expression in A549 cells after PEE treatment. (D) The p21 and cyclin E2 protein relative expression levels. Data were expressed as means  $\pm$  SD. \* $p < 0.05$ , \*\* $p < 0.01$ , \*\*\* $p < 0.001$  versus the control group.

revealed that the proportion of bright blue fluorescent cells with dense nuclei increased gradually after treatment with *P. puberula* root PEE, which had the characteristics of apoptosis.

The flow cytometry quantified the apoptosis induced by *P. puberula* root PEE using annexin V-PE/7-AAD staining (Fig. 5). Compared to the control group ( $7.04 \pm 0.95\%$ ), the percentage of apoptotic of A549 cells after being exposed to *P. puberula* root PEE at concentrations of 20, 40, 60, 80, and 100  $\mu\text{g/mL}$  increased to  $17.68 \pm 0.72\%$ ,  $58.66 \pm 0.87\%$ ,  $66.52 \pm 0.76\%$ ,  $86.60 \pm 0.08\%$ , and  $95.73 \pm 0.54\%$ , respectively. The above results showed that *P. puberula* root PEE induced apoptosis in A549 cells in a concentration-dependent manner.

### 3.6. The effect of *P. puberula* root PEE on mitochondrial membrane potential

Mitochondrial membrane potential ( $\Delta\Psi\text{m}$ ) is regarded as a fundamental parameter of mitochondrial function, and the downregulation of  $\Delta\Psi\text{m}$  is a characteristic event of apoptosis (Sivandzade et al., 2019). JC-1 fluorescent probe was utilized to detect  $\Delta\Psi\text{m}$ . In normal cells, JC-1 accumulates in the mitochondrial matrix to form polymers, yielding red fluorescence. However, in apoptotic cells, JC-1 can only exist as a monomer due to reduced or lost membrane potential, resulting in green

fluorescence. As shown in Fig. 6, along with the increase in the concentration of PEE administration, the proportion of cells showing red fluorescence gradually declined, and the proportion of cells showing green fluorescence progressively increased. The above results indicated that the *P. puberula* root PEE could reduce the mitochondrial membrane potential of A549 cells and induce cell apoptosis.

### 3.7. *P. puberula* root PEE induced apoptosis through the mitochondria apoptotic pathway

As  $\Delta\Psi\text{m}$  decreases, Cyt c is released into the cytoplasm, activating the caspase cascade reaction and ultimately induces apoptosis (Yu and Zhang, 2004). The western blot was applied to detect key proteins in mitochondrial-mediated apoptosis pathway. The levels of total Cyt c and mitochondrial Cyt c are depicted in Fig. 7A and B. The outcomes demonstrated that the level of mitochondria Cyt c was considerably down-regulated in a dose-dependent manner after treatment with *P. puberula* root PEE. In contrast, total Cyt c was markedly elevated, indicating that Cyt c was released from mitochondria.

As seen in Fig. 7C and D, *P. puberula* root PEE up-regulated Bax expression, while Bcl-2 was repressed, and the Bax/Bcl-2 ratio was significantly up-regulated in a dose-dependent manner. As depicted in

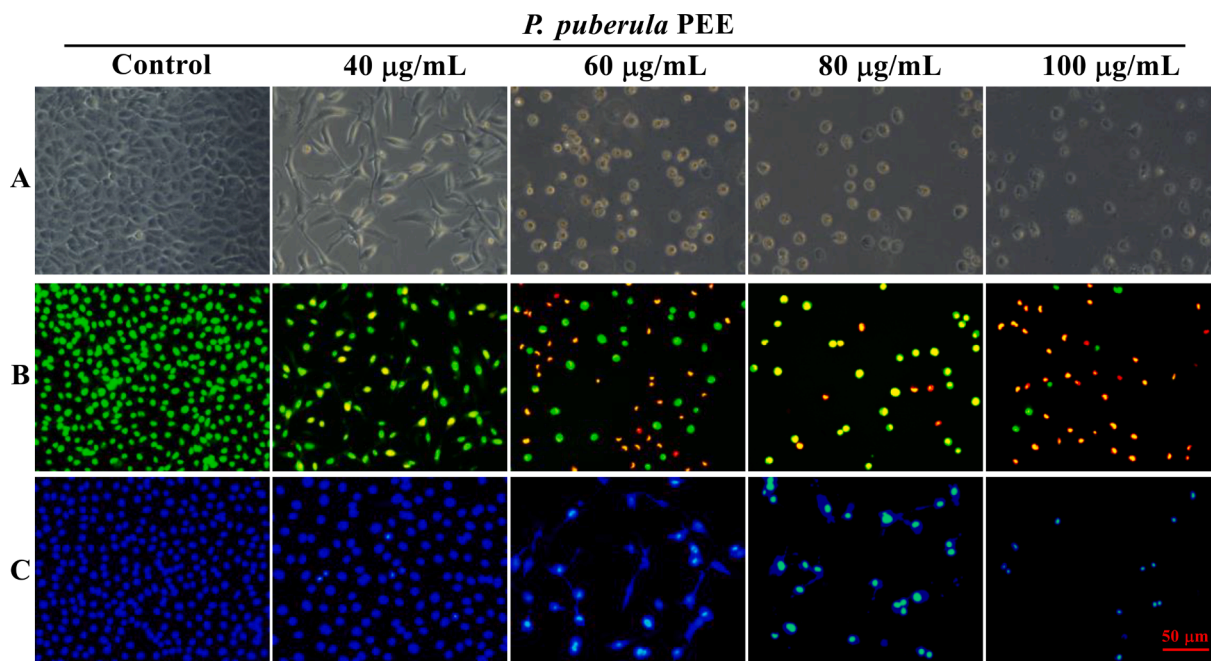


Fig. 4. The morphological changes of A549 cells exposed to various doses of *P. puberula* root PEE. (A) The A549 cells' morphological alterations under phase contrast microscope. (B, C) After staining with AO/EB (B) and Hoechst 33,258 (C), morphological changes of nuclei were observed under an inverted fluorescence microscope.

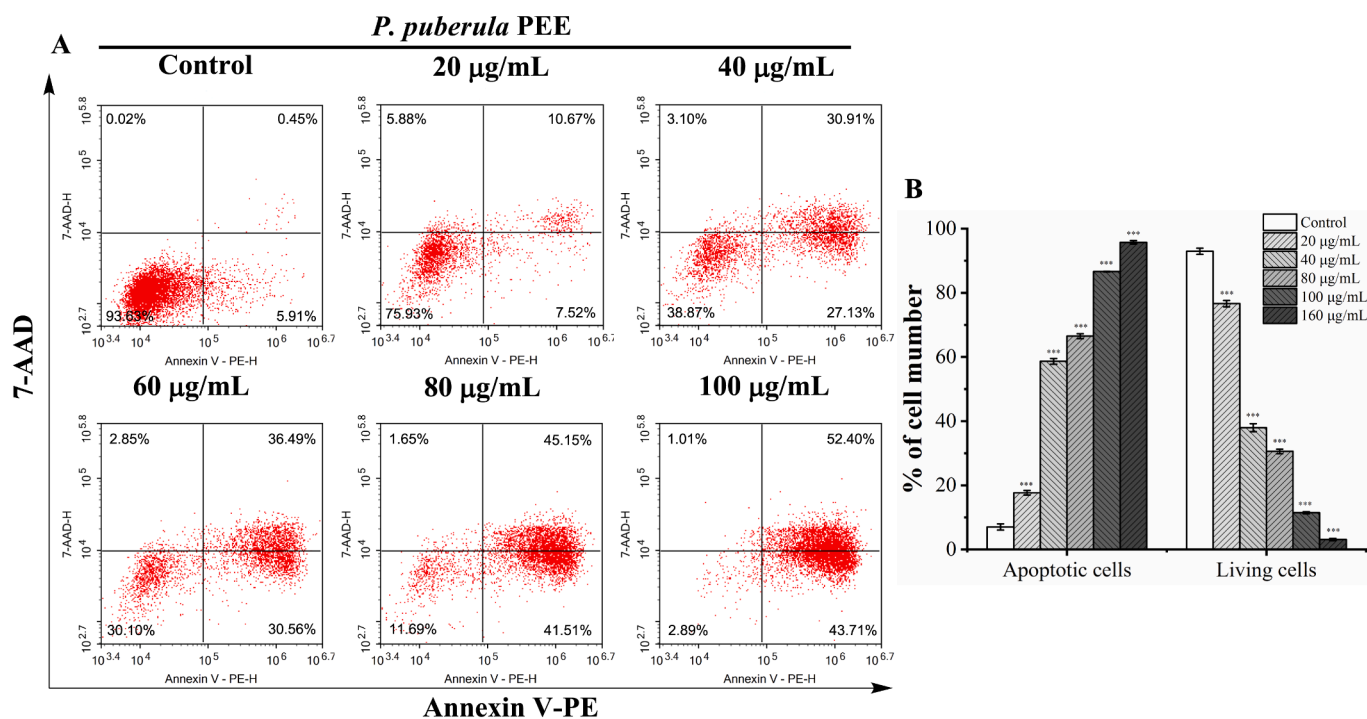


Fig. 5. The apoptosis of A549 cells treated with *P. puberula* root PEE was detected by a flow cytometer. (A) After treatment with the specified concentrations of *P. puberula* root PEE, A549 cells were labeled with Annexin V-PE and 7-AAD and then detected using a flow cytometer. Cells in upper right quadrant (AV+/7-AAD+): late apoptotic cells; lower right quadrant (AV+/7-AAD-): early apoptotic cells; upper left quadrant (AV-/7-AAD+): necrotic cells; lower left quadrant (AV-/7-AAD-): live cells. (B) The proportion of living and apoptotic cells. Data were expressed as means  $\pm$  SD. \*\*\* $p$  < 0.001 versus the control group.

Fig. 7C and E, *P. puberula* root PEE markedly declined the levels of pro-caspase 9 and pro-caspase 3 and up-regulated the levels of cleaved-caspase 9, cleaved-caspase 3, and cleaved-PARP, which suggested activation of the caspase cascade reaction, resulting in the cleavage of PARP. Thus, the *P. puberula* root PEE caused A549 cell apoptosis through the mitochondrial apoptotic pathway.

### 3.8. *P. puberula* root PEE inhibited the metastasis of A549 cells

The leading cause of death from cancer is metastasis from the initial site to other parts of the body (Duffy et al., 2008; Riihimäki et al., 2014). Wound healing assay and transwell invasion assay were performed to study the effect of *P. puberula* root PEE on the migration and invasion

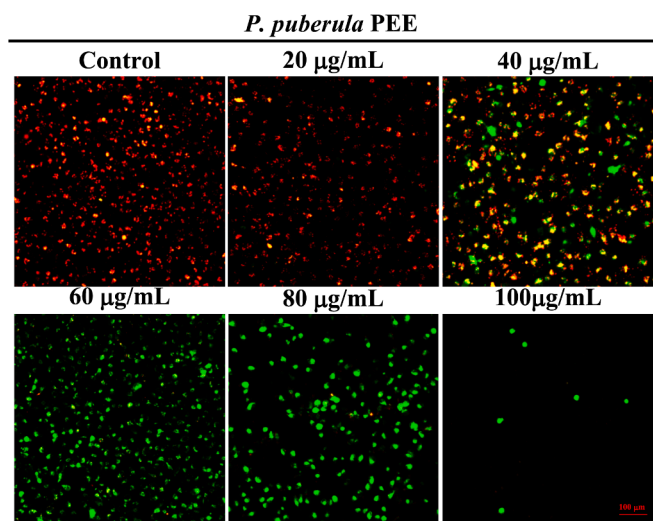


Fig. 6. The mitochondrial membrane potential of A549 cells treated with *P. puberula* root PEE. Cells were stained with JC-1 staining and imaged using an inverted fluorescence microscope.

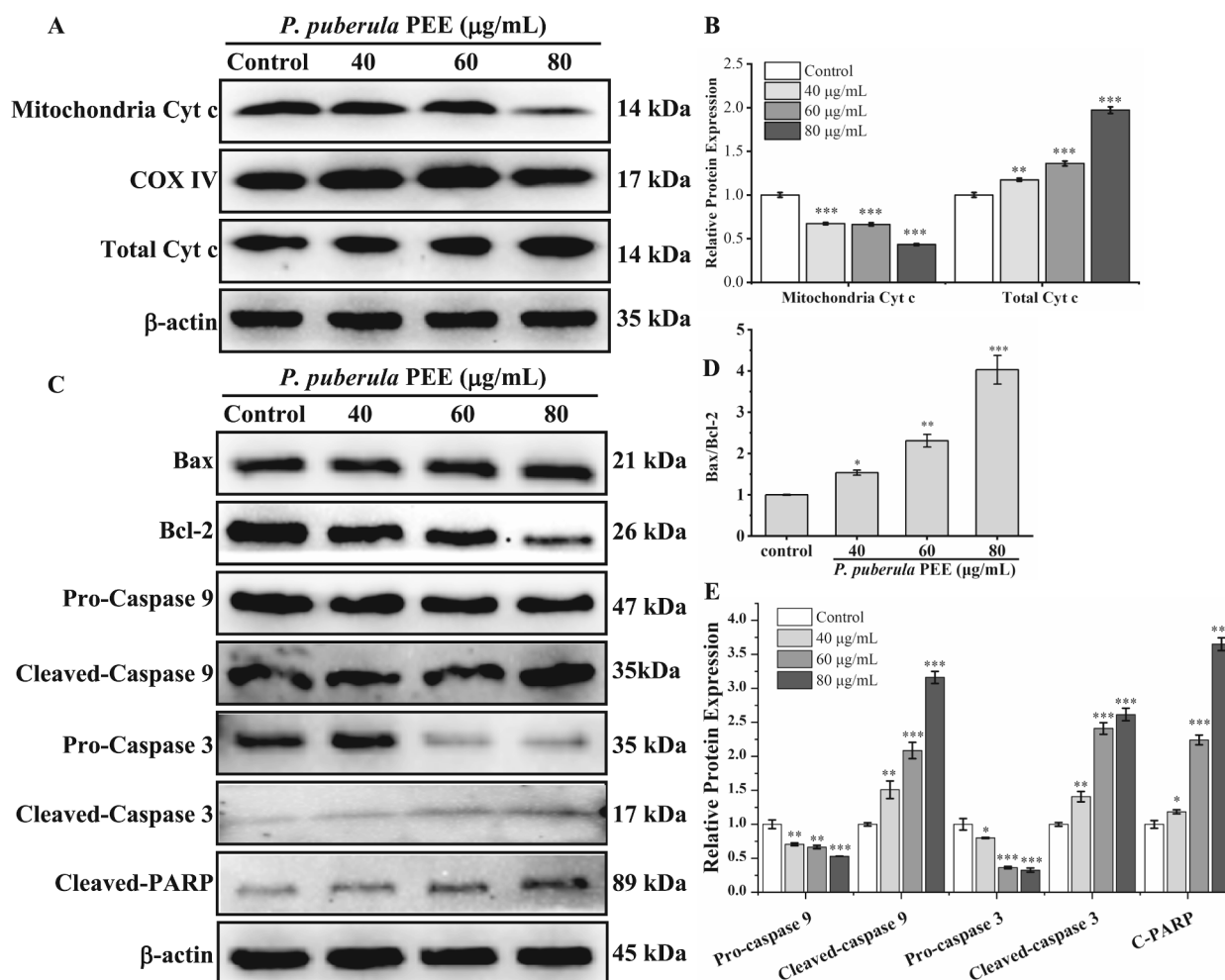


Fig. 7. The effect of *P. puberula* root PEE on A549 cells on mitochondrial apoptosis pathway-related proteins. (A, B) The total Cyt c and mitochondrial Cyt c protein levels in PEE-treated A549 cells were detected using a western blot. (C–E) Expression levels of Bax, Bcl-2, pro-caspase 9, cleaved-caspase 9, pro-caspase 3, cleaved-caspase 3, and cleaved-PARP proteins were detected by Western blot analysis. Data were expressed as means  $\pm$  SD. \* $p < 0.05$ , \*\* $p < 0.01$ , \*\*\* $p < 0.001$  versus the control group.

ability of A549 cells. Compared to the control group ( $73.92 \pm 0.83$  %), the migration rate of A549 cells treated with different concentrations (10, 20, and 30  $\mu\text{g/mL}$ ) of *P. puberula* root PEE observably reduced to  $48.65 \pm 1.29$  %,  $34.30 \pm 0.98$  %, and  $14.04 \pm 1.51$  %, respectively (Fig. 8A and B). Therefore, *P. puberula* root PEE signally and concentration-dependently inhibited the migratory capacity of A549 cells. The results of the transwell invasion assay (Fig. 8C and D) showed that *P. puberula* root PEE dramatically and dose-dependently decreased the number of invaded A549 cells compared to the control group, demonstrating that PEE inhibited A549 cells' invasive capacity.

The effect of *P. puberula* root PEE on metastasis-associated proteins was detected by western blot. As illustrated in Fig. 8E and F, *P. puberula* root PEE dramatically reduced the expression level of MMP-2. Besides, it down-regulated N-cadherin expression in a concentration-dependent manner. The above results suggested that *P. puberula* root PEE inhibited the migration and invasive ability of A549 cells by down-regulating MMP-2 and N-cadherin levels.

#### 4. Discussion

Various *Premna* plants have been demonstrated to possess anticancer activity. *P. serratifolia* extracts revealed cytotoxic activity against three cancer cells (A549, HepG2, and MCF-7); besides, *P. serratifolia* root aqueous extract induced ROS generation and mitochondria-mediated apoptosis and inhibited proliferation and migration of HepG2 cells

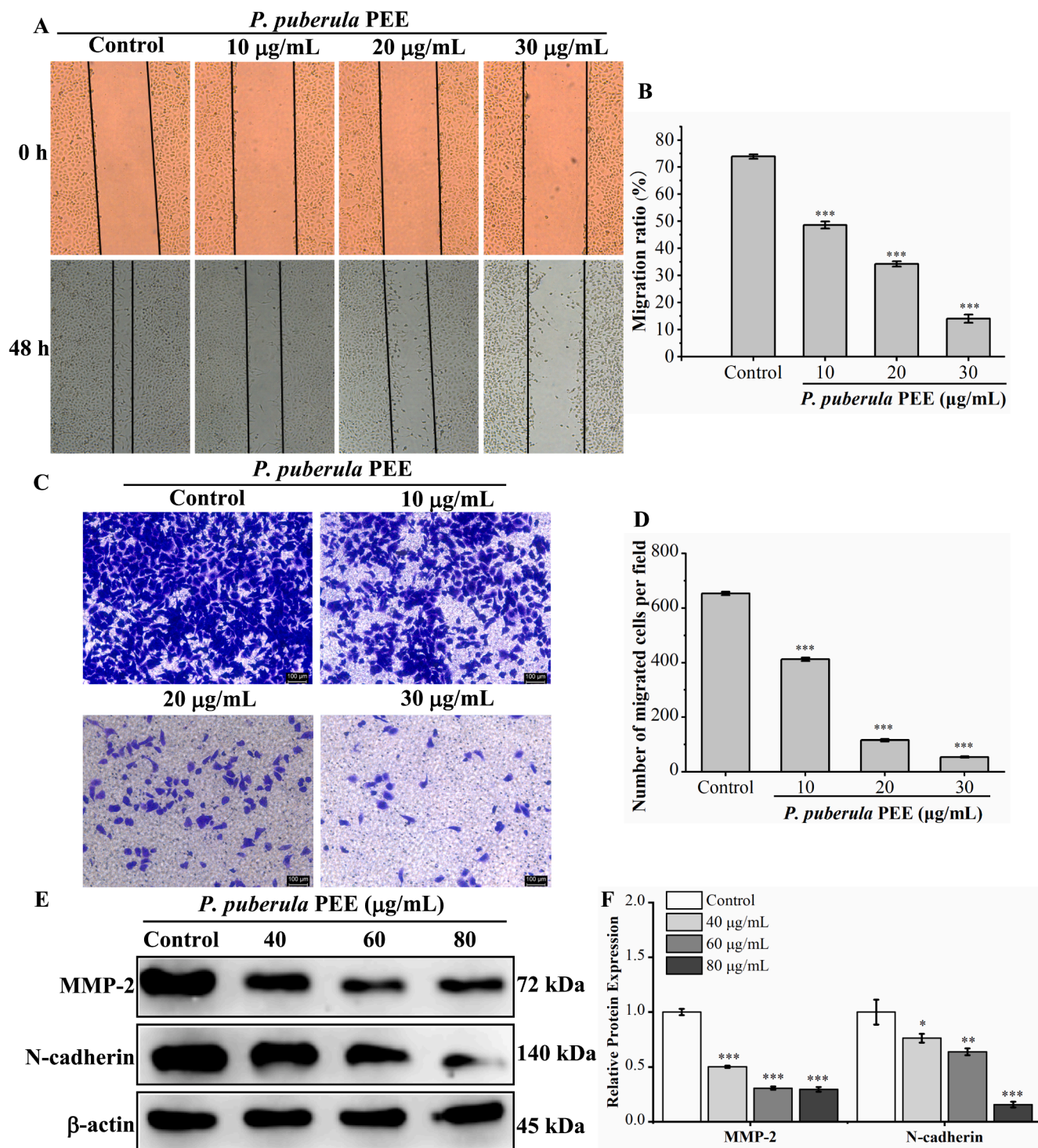


**Fig. 8.** The effect of *P. puberula* root PEE on migration and invasion and related protein expression in A549 cells. (A) Wound healing assay for detecting the migration ability of *P. puberula* root PEE on A549 cells. (B) Analysis of the migration capacity quantitatively using the migration ratio (%). (C) The invasive capacity was determined by the transwell invasion test ( $\times 100$ ). (D) The invasive ability was quantified. (E) Western blot detection of metastasis-associated protein (MMP-2, N-cadherin) expression in A549 cells after PEE treatment. (F) MMP-2 and N-cadherin proteins relative expression levels. Data were displayed as means  $\pm$  SD. Compared with the control group, \* $p < 0.05$ , \*\* $p < 0.01$ , \*\*\* $p < 0.001$ .

(Selvam et al., 2012; Singh et al., 2021). *P. odorata* leaves and bark extracts showed selectivity cytotoxicity to cancer cell lines (A549, HCT116, and MCF-7) and less toxicity to non-cancer cell line (Chinese hamster ovary AA8 cells) (Tantengco and Jacinto, 2015). *P. microphylla* aerial part essential oil exerted significant cytotoxic activity on HepG2 ( $\text{IC}_{50} = 0.072 \text{ mg/mL}$ ) and MCF-7 ( $\text{IC}_{50} = 0.188 \text{ mg/mL}$ ) cells (Zhang et al., 2017). *P. resinosa* aerial parts n-hexane extract had potent

cytotoxic effect on HepG2 ( $\text{IC}_{50} = 8.5 \pm 2.2 \mu\text{g/mL}$ ), Daoy ( $\text{IC}_{50} = 9.0 \pm 1.9 \mu\text{g/mL}$ ), and SK-MEL28 ( $\text{IC}_{50} = 13.2 \pm 4.1 \mu\text{g/mL}$ ) cancer cell lines (Albadawi et al., 2017).

According to the analysis of GC-FID/MS, the main components were ferruginol, cyclosativene, humulene epoxide II, pentacosane,  $\alpha$ -copaene, caryophyllene oxide, *o*-isopropylanisole, 1-docosene, dehydroabietan, and 3-eicosene. Ferruginol, as the main ingredient of *P. puberula* root

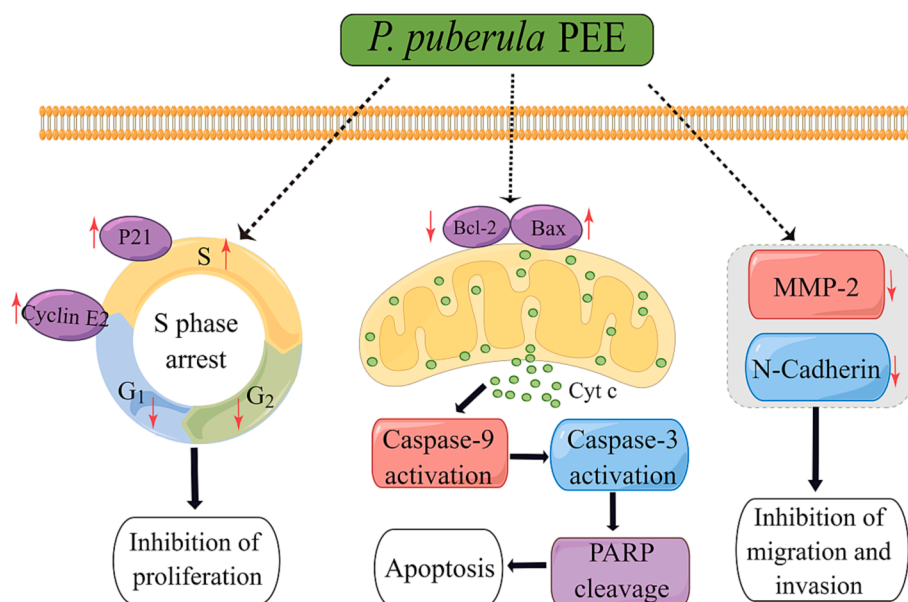


Fig. 9. Predicting anticancer mechanism of *P. puberula* root PEE on A549 cells.

PEE, had a cytotoxic effect on non-small cell lung cancer A549 and CL1-5 cells, induced apoptosis of A549 and CL1-5 through the caspase-dependent apoptosis pathway, and inhibited the growth of subcutaneous CL1-5 xenograft tumors (Ho et al., 2015). In addition, ferruginol had anticancer activity against human ovarian cancer OVCAR-3 cells, human malignant melanoma SK-Mel-28 cells, and prostate cancer PC-3 cells (Bispo et al., 2008; Jia et al., 2019; Xiong et al., 2017). Cyclosativene has been reported to possess anticancer properties and can serve as a potential antitumor agent (Lin et al., 2012; Toğar et al., 2014; Turkez et al., 2015). Furthermore, pentacosane (Mishra et al., 2019),  $\alpha$ -copaene (Turkez et al., 2014), caryophyllene oxide (Fidy et al., 2016; Pan et al., 2016; Park et al., 2011; Shabana et al., 2023), 1-docosene (Sneha and Varsha, 2018; Swantara et al., 2019) have been demonstrated to have antitumor activity. Therefore, the significant anticancer activity of *P. puberula* root PEE against A549 may be due to the important role played by these major chemical components.

*P. puberula* root PEE was significantly cytotoxic to A549 cells but less cytotoxic to the non-cancer cell line MRC-5. Therefore, the anticancer effects and associated mechanisms of *P. puberula* root PEE were further investigated. Cell cycle dysregulation is the main responsible for the malignant proliferation of cancer cells (Li et al., 2022). According to the findings of colony formation assay and cell cycle analysis, *P. puberula* root PEE inhibited the proliferation of A549 by arresting the cell cycle in the S phase. As a cell cycle protein-dependent kinase inhibitor, p21 inhibits cyclin A/CDK2 kinase activity, leading to cell cycle arrest in S phase (Karimian et al., 2016). Cyclin E is a key regulator of the transition from G1 to S phase (Mishina et al., 2000). Our results showed that the *P. puberula* root PEE induced S cell cycle arrest by up-regulating p21 and cyclin E2 levels.

An important hallmark of tumors is the ability to avoid cell death (Sun et al., 2020). In this study, the observation results of the nucleus morphology and cell morphology of A549 cells indicated that A549 cells treated with *P. puberula* root PEE showed typical cytomorphological changes such as nuclear chromatin condensation, cell rounding, and shrinkage. At the same time, flow cytometry detection further revealed that *P. puberula* root PEE dose-dependently induced apoptosis in A549 cells. In the mitochondrial apoptotic pathway, Bcl-2 family proteins are crucial apoptosis regulators, which accumulate on mitochondria to induce outer mitochondrial membrane permeation and then trigger the down-regulation of  $\Delta\Psi_m$  and the release of Cyt c (Green and Kroemer, 2004; Meng et al., 2017; Renault et al., 2015). Bcl-2 family proteins

include anti-apoptotic proteins (Bcl-2, Bcl-XL) and pro-apoptotic proteins (Bax, Bak), and increasing the ratio between pro-apoptotic proteins and anti-apoptotic proteins, such as Bax/Bcl-2, induces apoptosis (Chen et al., 2007; Hayakawa et al., 2016; Kale et al., 2018). Released Cyt c causes cleavage of caspase-9, caspase-3, and PARP, leading to apoptosis of cancer cells (Zhang et al., 2011). In the JC-1 staining assay, the *P. puberula* root PEE reduced  $\Delta\Psi_m$  in A549 cells, which indicated that the *P. puberula* root PEE induced apoptosis through the mitochondria-mediated apoptotic pathway. Therefore, this study investigated the protein levels involved in the mitochondrial apoptotic pathway. The results showed that *P. puberula* root PEE increased the Bax/Bcl-2 ratio, decreased  $\Delta\Psi_m$ , and prompted the release of Cyt c into the cytoplasm, thereby cleaving and activating caspase-9 and caspase-3, which then cleaved PARP and ultimately led to apoptotic cell death. The above results suggest that *P. puberula* root PEE induced apoptosis in A549 cells through the mitochondrial pathway.

Cancer metastasis includes the migration and invasion of cancer cells, which is the leading cause of cancer death (Deborde et al., 2022). As a matrix metalloproteinase (MMP), MMP-2 breaks through the structural barrier of cancer cell metastasis by degrading type IV collagen, a primary substrate membrane component (Song et al., 2013). The high expression of N-cadherin in cancer can facilitate the migration of cancer cells and increase the invasion ability to the basement membrane, so reducing the expression of N-cadherin can inhibit the metastasis of cancer cells (Klein and Bischoff, 2011). Therefore, this study investigated the expression of MMP-2 and N-cadherin. The results showed that the *P. puberula* root PEE down-regulated the expression of MMP-2 and N-cadherin, thus inhibiting the migration and invasion capacity of A549 cells.

In conclusion, in the present study, we first reported that *P. puberula* root PEE possesses significant antitumor activity, which can inhibit the proliferation of A549 cells, induce apoptosis by mitochondria-mediated pathway, and suppress migration and invasion. As shown in Fig. 9, *P. puberula* root PEE arrested the cell cycle in the S phase by up-regulating p21 and cyclin E2 expression to inhibit the proliferation of A549 cells. Meanwhile, it triggered apoptosis by the mitochondrial pathway, with elevated Bax/Bcl-2 ratio, decreased  $\Delta\Psi_m$ , release of Cyt c, activation of caspase-9 and caspase-3, and cleavage of PARP. Besides, *P. puberula* root PEE suppressed A549 cell migration and invasion by down-regulating MMP-2 and N-cadherin. These data indicate that *P. puberula* root PEE has excellent anticancer activity *in vitro*. These

discoveries provide the basis for the exploitation of *P. puberula* root PEE as an anticancer agent in the pharmaceutical industry.

## 5. Conclusion

The chemical composition of *P. puberula* root PEE and its anticancer properties and related mechanisms were reported for the first time in this study. GC-FID/MS analysis indicated that the main constituents of *P. puberula* root PEE were ferruginol, cyclosativene, humulene epoxide II, pentacosane,  $\alpha$ -copaene, caryophyllene oxide, *o*-isopropylanisole, 1-docosene, dehydroabietan, and 3-icosene. In terms of antitumor activity, *P. puberula* root PEE exhibited selective cytotoxicity to A549 cells and less toxicity to normal cell MRC-5. In addition, *P. puberula* root PEE inhibited proliferation by arresting cells at the S phase, induced apoptosis by mitochondria-mediated pathway, and suppressed migration and invasion of A549 cells. Therefore, *P. puberula* root PEE has outstanding anticancer properties *in vitro* and can be a new source of antitumor agents.

## CRedit authorship contribution statement

**Nian Yang:** Investigation, Methodology, Resources, Validation. **Xiaoyan Jia:** Investigation, Methodology, Resources, Validation. **Yao Yang:** Investigation, Methodology. **Jingming Niu:** Investigation. **Xia Wu:** Validation. **Furong Ding:** Resources, Validation. **Minyi Tian:** Methodology, Validation, Supervision, Writing – original draft, Writing – review & editing, Funding acquisition. **Dongxin Tang:** Conceptualization, Writing – review & editing, Funding acquisition.

## Declaration of competing interest

The authors declare that they have no known competing financial interests or personal relationships that could have appeared to influence the work reported in this paper.

## Acknowledgment

The authors are grateful for the financial support grant from the National Natural Science Foundation of China (82360834) and Science and Technology Program of Guizhou province, China [Qian Ke He Zhi Cheng (2020) 1Y133, Qian Ke He Ji Chu-ZK (2021) Yiban 150].

## References

Albadawi, D.A., Mothana, R.A., Khaled, J.M., Ashour, A.E., Kumar, A., Ahmad, S.F., Al-Said, M.S., Al-Rehaily, A.J., Almusaeyb, N.M., 2017. Antimicrobial, anticancer, and antioxidant compounds from *Premna resinosa* growing in Saudi Arabia. *Pharm. Biol.* 55 (1), 1759–1766.

Atanasov, A.G., Zotchev, S.B., Dirsch, V.M., Supuran, C.T., 2021. Natural products in drug discovery: advances and opportunities. *Nat. Rev. Drug Discov.* 20, 200–216.

Bispo de Jesus, M., Zambuzzi, W.F., Ruela de Sousa, R.R., Areche, C., Santos de Souza, A. C., Aoyama, H., Schmeda-Hirschmann, G., Rodríguez, J.A., de Souza, M., Brito, A.R., Peppelenbosch, M.P., den Hertog, J., de Paula, E., Ferreira, C.V., 2008. Ferruginol suppresses survival signaling pathways in androgen-independent human prostate cancer cells. *Biochimie* 90, 843–854.

Chen, S.L., Gilbert, M.G., 1994. Verbenaceae. In: Wu, Z.Y., Raven, P.H. (Eds.), *Flora of China*, Vol. 17. Science Press, Beijing & Missouri Botanical Garden Press, St. Louis, pp. 1–49.

Chen, Y., Haviernik, P., Bunting, K.D., Yang, Y.C., 2007. Cited2 is required for normal hematopoiesis in the murine fetal liver. *Blood* 110 (8), 2889–2898.

Chinese Materia Medica Editorial Committee, 1999. *Zhong Hua Ben Cao* [Chinese Materia Medica]. Shanghai Science and Technology Press, Shanghai, China 6, 587–589.

Deborde, S., Gusain, L., Powers, A., Marcadis, A., Yu, Y., Chen, C.H., Frants, A., Kao, E., Tang, L.H., Vakiani, E., Amisaki, M., Balachandran, V.P., Calo, A., Omelchenko, T., Jessen, K.R., Reva, B., Wong, R.J., 2022. Reprogrammed Schwann Cells Organize into Dynamic Tracks that Promote Pancreatic Cancer Invasion. *Cancer Discov.* 12, 2454–2473.

Diaz-Moralli, S., Tarrado-Castellarnau, M., Miranda, A., Cascante, M., 2013. Targeting cell cycle regulation in cancer therapy. *Pharmacol Ther.* 138, 255–271.

Duffy, M.J., McGowan, P.M., Gallagher, W.M., 2008. Cancer invasion and metastasis: changing views. *J. Pathol.* 214, 283–293.

Fidy, K., Fiedorowicz, A., Strzȳda, L., Szumny, A., 2016.  $\beta$ -caryophyllene and  $\beta$ -caryophyllene oxide-natural compounds of anticancer and analgesic properties. *Cancer Med.* 5 (10), 3007–3017.

Fu, L.X., Ding, F.R., Ren, N., Jia, X.Y., Tian, M.Y., Deng, G.D., Wang, H.J., 2023. *In vitro* anti-inflammatory activities of essential oil from *Premna Puberula* Pamp. Stem and mechanism study based on NF- $\kappa$ B and MAPKs signaling pathways. *Chin. J. Hosp. Pharm.* 43 (1), 34–41.

Godoy, L.A., Chen, J., Ma, W., Lally, J., Toomey, K.A., Rajappa, P., Sheridan, R., Mahajan, S., Stollenwerk, N., Phan, C.T., Cheng, D., Knebel, R.J., Li, T., 2023. Emerging precision neoadjuvant systemic therapy for patients with resectable non-small cell lung cancer: current status and perspectives. *Biomark. Res.* 11, 7.

Green, D.R., Kroemer, G., 2004. The Pathophysiology of Mitochondrial Cell Death. *Science* 305 (5684), 626–629.

Hayakawa, K., Formica, A.M., Brill-Dashoff, J., Shinton, S.A., Ichikawa, D., Zhou, Y., Morse, H.C.I., Hardy, R.R., 2016. Early generated B1 B cells with restricted BCRs become chronic lymphocytic leukemia with continued c-Myc and low Bmf expression. *J. Exp. Med.* 213 (13), 3007–3024.

Ho, S.T., Tung, Y.T., Kuo, Y.H., Lin, C.C., Wu, J.H., 2015. Ferruginol Inhibits Non-Small Cell Lung Cancer Growth by Inducing Caspase-Associated Apoptosis. *Integr. Cancer Ther.* 14 (1), 86–97.

Hong, Y., Liu, X., Wang, H., Zhang, M., Tian, M., 2022. Chemical composition, anticancer activities and related mechanisms of the essential oil from *Alpinia coriandrorhiza* rhizome. *Ind. Crop. Prod.* 176, 114328.

Huang, M., Lu, J.J., Huang, M.Q., Bao, J.L., Chen, X.P., Wang, Y.T., 2012. Terpenoids: natural products for cancer therapy. *Expert Opin. Investig. Drugs.* 21 (12), 1801–1818.

Hung, N.H., Huong, L.T., Chung, N.T., Truong, N.C., Dai, D.N., Satyal, P., Tai, T.A., Hien, V.T., Setzer, W.N., 2020. *Premna* Species in Vietnam: Essential Oil Compositions and Mosquito Larvicidal Activities. *Plants* 9, 1130.

Jia, Y., Wu, C., Zhang, B., Zhang, Y., Li, J., 2019. Ferruginol induced apoptosis on SK-Mel-28 human malignant melanoma cells mediated through P-p38 and NF- $\kappa$ B. *Hum. Exp. Toxicol.* 38 (2), 227–238.

Kale, J., Osterlund, E.J., Andrews, D.W., 2018. BCL-2 family proteins: changing partners in the dance towards death. *Cell Death Differ.* 25, 65–80.

Karimian, A., Ahmadi, Y., Yousefi, B., 2016. Multiple functions of p21 in cell cycle, apoptosis and transcriptional regulation after DNA damage. *DNA Repair* 42, 63–71.

Klein, T., Bischoff, R., 2011. Physiology and pathophysiology of matrix metalloproteinases. *Amino Acids* 41, 271–290.

Koehn, F.E., Carter, G.T., 2005. The evolving role of natural products in drug discovery. *Nat. Rev. Drug Discov.* 4, 206–220.

Li, Y.Q., Liu, Y.L., Luo, X.J., Liu, L., Yuan, G.X., Fang, X.P., 2016. Evaluation of *Premna* Linn. Plants Based on Multi-factor Rating Weighted Index Summation Method. *Mol. Plant Breed.* 14 (6), 1631–1636.

Li, H., Zhong, Y., Cao, G., Shi, H., Liu, Y., Li, L., Yin, P., Chen, J., Xiao, Z., Du, B., 2022. METTL3 promotes cell cycle progression via m<sup>6</sup>A/YTHDF1-dependent regulation of *CDC25B* translation. *Int. J. Biol. Sci.* 18 (8), 3223–3236.

Lin, J., Dou, J., Xu, J., Aisa, H.A., 2012. Chemical Composition, Antimicrobial and Antitumor Activities of the Essential Oils and Crude Extracts of *Euphorbia macrorrhiza*. *Molecules* 17, 5030–5039.

Liu, K., Guo, Y., Chen, X., Duan, J., Li, B., Liu, M., Chen, L., Li, M., Feng, Y., Li, H., Wang, X., 2022. Quality control, preparation process optimizing and anti-inflammatory effects of *Premna Puberula* Pamp. Pectin. *Heliyon* 8, e11082.

Meng, H., Yamashita, C., Shiba-Fukushima, K., Inoshita, T., Funayama, M., Sato, S., Hatta, T., Natsume, T., Umitsu, M., Takagi, J., Imai, Y., Hattori, N., 2017. Loss of Parkinson's disease-associated protein CHCHD2 affects mitochondrial cristae structure and destabilizes cytochrome c. *Nat. Commun.* 8, 15500.

Mishina, T., Dosaka-Akita, H., Hommura, F., Nishi, M., Kojima, T., Ogura, S., Shimizu, M., Katoh, H., Kawakami, Y., 2000. Cyclin E Expression, a Potential Prognostic Marker for Non-Small Cell Lung Cancers. *Clin. Cancer Res.* 6, 11–16.

Mishra, S., Verma, S.S., Rai, V., Awasthee, N., Arya, J.S., Maiti, K.K., Gupta, S.C., 2019. *Curcuma raktakanda* Induces Apoptosis and Suppresses Migration in Cancer Cells: Role of Reactive Oxygen Species. *Biomolecules* 9, 159.

Pan, Z., Wang, S.K., Cheng, X.L., Tian, X.W., Wang, J., 2016. Caryophyllene oxide exhibits anti-cancer effects in MG-63 human osteosarcoma cells via the inhibition of cell migration, generation of reactive oxygen species and induction of apoptosis. *Bangladesh J. Pharmacol.* 11, 817–823.

Park, K.R., Nam, D., Yun, H.M., Lee, S.G., Jang, H.J., Sethi, G., Cho, S.K., Ahn, K.S., 2011.  $\beta$ -Caryophyllene oxide inhibits growth and induces apoptosis through the suppression of PI3K/AKT/mTOR/S6K1 pathways and ROS-mediated MAPKs activation. *Cancer Lett.* 312, 178–188.

Renault, T.T., Floros, K.V., Elkholi, R., Corrigan, K.A., Kushnareva, Y., Wieder, S.Y., Lindtner, C., Serasinghe, M.N., Ascioffa, J.J., Buettnert, C., Newmeyer, D.D., Chipuk, J.E., 2015. Mitochondrial Shape Governs BAX-Induced Membrane Permeabilization and Apoptosis. *Mol. Cell* 57, 69–82.

Riihimäki, M., Hemminki, A., Fallah, M., Thomsen, H., Sundquist, K., Sundquist, J., Hemminki, K., 2014. Metastatic sites and survival in lung cancer. *Lung Cancer* 86, 78–84.

Selvam, T.N., Venkatakrishnan, V., Damodar, K.S., Elumalai, P., 2012. Antioxidant and Tumor Cell Suppression Potential of *Premna Serratifolia* Linn Leaf. *Toxicol. Int.* 19, 31–34.

Shabana, S.M., Gad, N.S., Othman, A.I., Mohamed, A.F., El-Missiry, M.A., 2023.  $\beta$ -caryophyllene oxide induces apoptosis and inhibits proliferation of A549 lung cancer cells. *Med. Oncol.* 40, 189.

She, G., Du, J.C., Wu, W., Pu, T.T., Zhang, Y., Bai, R.Y., Zhang, Y., Pang, Z.D., Wang, H.F., Ren, Y.J., Sadoshima, J., Deng, X.L., Du, X.J., 2023. Hippo pathway activation

- mediates chemotherapy-induced anti-cancer effect and cardiomyopathy through causing mitochondrial damage and dysfunction. *Theranostics* 13 (2), 560–577.
- Siegel, R.L., Miller, K.D., Wagle, N.S., Jemal, A., 2023. Cancer statistics, 2023. *CA Cancer J. Clin.* 73, 17–48.
- Singh, C., Anand, S.K., Tiwari, K.N., Mishra, S.K., Kakkar, P., 2021. Phytochemical Profiling and Cytotoxic Evaluation of *Premna Serratifolia* L. against Human Liver Cancer Cell Line. *3 Biotech* 11, 115.
- Sivandzade, F., Bhalerao, A., Cucullo, L., 2019. Analysis of the Mitochondrial Membrane Potential Using the Cationic JC-1 Dye as a Sensitive Fluorescent Probe. *Bio Protoc.* 9 (1), e3128.
- Sneha, S.S., Varsha, K.M., 2018. Nutritional profile, antioxidant, antimicrobial potential, and bioactives profile of *Chlorella emersonii* KJ725233. *Asian J. Pharm. Clin. Res.* 11 (3), 220–225.
- Song, N.R., Hwang, M.K., Heo, Y.S., Lee, K.W., Lee, H.J., 2013. Piceatannol suppresses the metastatic potential of MCF10A human breast epithelial cells harboring mutated H-ras by inhibiting MMP-2 expression. *Int. J. Mol. Med.* 32, 775–784.
- Sun, G., Ding, X.A., Argaw, Y., Guo, X., Montell, D.J., 2020. Akt1 and dCIZ1 promote cell survival from apoptotic caspase activation during regeneration and oncogenic overgrowth. *Nat. Commun.* 11, 5726.
- Sung, H., Ferlay, J., Siegel, R.L., Laversanne, M., Soerjomataram, I., Jemal, A., Bray, F., 2021. Global Cancer Statistics 2020: GLOBOCAN Estimates of Incidence and Mortality Worldwide for 36 Cancers in 185 Countries. *CA Cancer J. Clin.* 71, 209–249.
- Swantara, M.D., Rita, W.S., Suartha, N., Agustina, K.K., 2019. Anticancer activities of toxic isolate of *Xestospongia testudinaria* sponge. *Vet. World* 12 (9), 1434–1440.
- Tantengco, O.A.G., Jacinto, S.D., 2015. Cytotoxic activity of crude extracts and fractions from *Premna odorata* (Blanco), *Artocarpus camansi* (Blanco) and *Gliricidia sepium* (Jacq.) against selected human cancer cell lines. *Asian Pac. J Trop. Biomed.* 5 (12), 1037–1041.
- Tian, M.Y., Wu, X.H., Lu, T.Y., Zhao, X.G., Wei, F., Deng, G.D., Zhou, Y., 2020. Phytochemical Analysis, Antioxidant, Antibacterial, Cytotoxic, and Enzyme Inhibitory Activities of *Hedychium flavum* Rhizome. *Front. Pharmacol.* 11, 572659.
- Togar, B., Türkez, H., Geyikoglu, F., Hacimuftuoglu, A., Tatar, A., 2014. Antiproliferative, genotoxic and oxidant activities of cyclosativene in rat neuron and neuroblastoma cell lines. *Arch. Biol. Sci.* 66 (3), 1171–1177.
- Turkez, H., Togar, B., Tatar, A., Geyikoglu, F., Hacimuftuoglu, A., 2014. Cytotoxic and cytogenetic effects of  $\alpha$ -copaene on rat neuron and N2a neuroblastoma cell lines. *Biologia* 69 (7), 936–942.
- Turkez, H., Togar, B., Di Stefano, A., Taspinar, N., Sozio, P., 2015. Protective effects of cyclosativene on H<sub>2</sub>O<sub>2</sub>-induced injury in cultured rat primary cerebral cortex cells. *Cytotechnology* 67, 299–309.
- WFO, 2023. *Premna puberula* Pamp. Available online: <https://www.worldfloraonline.org/taxon/wfo-0000282794> (accessed on 31 August 2023).
- Xiong, W.D., Gong, J., Xing, C., 2017. Ferruginol exhibits anticancer effects in OVCAR-3 human ovary cancer cells by inducing apoptosis, inhibition of cancer cell migration and G2/M phase cell cycle arrest. *Mol. Med. Rep.* 16, 7013–7017.
- Xu, L., Shi, M.N., Zhang, M.S., 2011. Preliminary Investigation of Cutting Propagation in *Premna Puberula* Pamp. *J. MT. Agric. Biol.* 30 (1), 82–86.
- Yang, N.X., Wang, D.P., Geng, Y.Y., Man, J.M., Gao, Y.Y., Hang, Y., Zheng, H.J., Zhang, M.S., 2022. Structure, physicochemical characterisation and properties of pectic polysaccharide from *Premna puberula* pamp. *Food Hydrocoll.* 128, 107550.
- Ye, H., Li, C., Ye, W., Zeng, F., Liu, F., Liu, Y., Wang, F., Ye, Y., Fu, L., Li, J., 2022. Medicinal Angiosperms of Verbenaceae. In: Ye, H., Li, C., Ye, W., Zeng, F. (Eds.), *Common Chinese Materia Medica*. Springer, Singapore, pp. 440–441.
- Yu, J., Zhang, L., 2004. Apoptosis in human cancer cells. *Curr. Opin. Oncol.* 16, 19–24.
- Zhang, H.Y., Gao, Y., Lai, P.X., 2017. Chemical Composition, Antioxidant, Antimicrobial and Cytotoxic Activities of Essential Oil from *Premna microphylla* Turczaninow. *Molecules* 22, 381.
- Zhang, H., Li, Y., Huang, Q., Ren, X., Hu, H., Sheng, H., Lai, M., 2011. MiR-148a promotes apoptosis by targeting Bcl-2 in colorectal cancer. *Cell Death Differ.* 18, 1702–1710.
- Zhang, M.S., Shi, M.N., Xu, B.R., Li, X.D., Cao, R., Chen, L., 2012. A Key Component Determination on Forming Fairy Tofu from the Leaf of *Premna Puberula* (Verbenaceae). *J. Appl. Pharmaceut. Sci.* 2 (9), 031–035.